Water Orientation at Hydrophobic Interfaces

Simona Strazdaite,[1] Jan Versluis,[1] and Huib J. Bakker[1]

FOM Institute AMOLF, Science Park 104, 1098 XG Amsterdam, The Netherlands

(Dated: 27 August 2015)

We study the structure and orientation of water molecules at water/alkane and water/polydimethylsiloxane interfaces with surface specific intensity and heterodyne-detected vibrational sum-frequency generation (HD-VSFG) spectroscopy. We observe that the hydrogen-bond structure of the water molecules is enhanced at these interfaces compared to the water/air interface. We also find that the water molecules at the interface show a net orientation of their O-H groups pointing towards to the hydrophobic layer.

PACS numbers: 78.47.N-

I. INTRODUCTION

The structure of water solvating hydrophobic solutes has been debated for almost 70 years. The discussions started with the 'iceberg' model proposed by Frank and Evans[1]. This model was inspired by thermodynamic measurements that showed that the associated entropy of solvation of hydrophobic molecular groups was negative, pointing to an enhanced ordering of the water molecules surrounding the hydrophobe. Based on these observations Frank and Evans suggested that water solvating a hydrophobic solute would acquire an ice-like structure. This model was later disputed by neutron scattering experiments[2,3] that rather found the pair correlation function of water around hydrophobic solutes to be similar to that of bulk liquid water. Theoretical work, in particular by Chandler and co-workers, did find that the hydrogen bond network of water surrounding small hydrophobic solute (<1 nm) remains intact, whereas for water surrounding large hydrophobic solutes the hydrogen-bonding network becomes disrupted[4,5].

Recently, a few experimental studies have been reported providing information on the structure and ordering of water near hydrophobic molecular groups. In a recent Raman scattering study evidence was found for an enhanced tetrahedral ordering of water molecules around small hydrophobic solutes[6]. An excellent surface-specific technique to study the properties of water molecules at aqueous interfaces is vibrational surface sum-frequency generation (VSFG) spectroscopy.

In VSFG spectroscopy an infrared (IR) beam and a visible (VIS) beam are combined at an interface to generate light at their sum frequency. The generated SFG electric field depends on the second-order non-linear susceptibility $\chi^{(2)}$ and the incoming visible (E_{VIS}) and infrared (E_{IR}) electric field strengths:

$$I_{SFG} = \mid E_{SFG} \mid^2 \approx \mid \chi^{(2)} E_{VIS} E_{IR} \mid^2 \tag{1}$$

The sum frequency signal is enhanced when the IR beam is resonant with a molecular vibration at the interface. VSFG derives its surface specificity from the fact that a molecular vibration is only SFG active in case it possesses a net orientation (breaking of symmetry). Water molecules in the bulk are isotropically oriented, and as a result there is no net VSFG signal generated from the bulk[11,12].

The frequency spectrum of the molecular vibrations and the orientation of the transition dipoles is contained in $\chi^{(2)}$ which in turn is determined by the molecular hyperpolarizabilities

(β) of the molecules at the interface[13]:

$$\chi^{(2)}_{ijk} = \sum_{i'j'k'} (N_s \beta_{i'j'k'} R(\langle \cos\theta \rangle, \langle \cos^3\theta \rangle)) \tag{2}$$

where *ijk* denotes Cartesian lab frame coordinates, and *i'j'k'* - molecular frame coordinates. N_s is number of molecules probed at the interface and R is the orientation function, which depends on $\langle \cos\theta \rangle$ and $\langle \cos^3\theta \rangle$, where θ is the polar angle with respect to the surface normal. The sign of $\chi^{(2)}$ is determined by the orientation of the molecules at the interface (θ).

In most VSFG spectroscopic experiments the intensity of the sum-frequency light is detected, which gives only the absolute square of the electric field $|E_{SFG}|^2$. Hence, in these intensity VSFG experiments, the sign (phase) of $\chi^{(2)}$ is not known, and thus the information on the orientation of the molecules is lost. Information on the orientation can be obtained using interference based heterodyne-detected vibrational sum-frequency generation (HD-VSFG) spectroscopy[13–15]. In this technique the VSFG electric field is combined with a local oscillator electric field at the same frequency of known phase:

$$\begin{aligned} I_{SFG} = &\mid E_{LO} + E_{Sample} \mid^2 = \mid E_{LO} \mid^2 + \mid E_{Sample} \mid^2 \\ &+ E_{LO} E^*_{Sample} + E^*_{LO} E_{Sample} \end{aligned} \tag{3}$$

The final detected VSFG intensity contains cross terms from which the real and imaginary part of $\chi^{(2)}$ can be extracted.

The group of Shen used HD-VSFG to study the orientation of water molecules at a fused quartz surface covered with an octadecyltrichlorosilane (OTS) monolayer[7]. The low-frequency water hydroxyl vibrations were observed to show an enhanced net orientation away from the bulk in comparison to a water/air interface. This enhanced net orientation was explained from the presence of hydroxide ions at the interface of water and the hydrophobic tails of the OTS monolayer. However, in another study of the same Quartz/OTS/water system, the changes in the VSFG spectra were attributed to the water molecules that are adsorbed near the polar head groups of the OTS molecules and the quartz surface[8]. In a very recent work by the group of Tyrode et al. it was shown that the SFG response of water near an OTS coated silica surface strongly depends on the quality of the self-assembled OTS layer[9]. The signal increase of the hydrogen-bonded water molecules observed for some of the self-assembled OTS layers was assigned to water directly interacting with the fused silica substrate.

The orientation of water molecules at an oil interface has also been investigated by probing the surface of oil droplets immersed in water with VSFG scattering spectroscopy[10]. In this study information on the orientation of the water molecules was obtained from the interference of the response of the C-H stretch vibrations of the oil with the low-frequency tail of the water hydroxyl vibrations. This interference was observed to be the same at the interface of a neutral oil droplet as at an interface covered with a negatively charged surfactant, which indicated that the water molecules are preferentially oriented with their hydroxyl groups pointing to the hydrophobic droplets. However, the main response of the water hydroxyl vibration could not be observed because of the strong infrared absorption of the water phase embedding the oil droplets. Interesting open questions are thus whether all water molecules show the same net orientation at a hydrophobic interface and how the orientation depends on the shape (curvature) and nature of the hydrophobic medium.

Here we present intensity VSFG and HD-VSFG studies of the ordering and hydrogen-bonding of water molecules at water/hexane, water/heptane and water/polydimethylsiloxane interfaces. We find evidence that the structure of water at these interfaces is enhanced compared to the structure of water at a water/air interface. Further, we find that the water molecules have a preferred orientation with their dipole moments pointing to hydrophobic layer.

II. EXPERIMENTAL

Our experimental setup for intensity SFG measurements have been described in details previously[20]. The experimental geometry of HD-VSFG setup is shown in figure 1. We generate an intense broad-band mid-IR pulse with a central wavelength of 4 μm via parametric amplification and difference frequency generation using the intense 800 nm pulses of a Ti:sapphire amplifier laser system as input. The generated 4 μm pulses have an energy of 10 μJ, a spectral bandwidth of $\sim$300 cm^{-1} and a pulse duration of $\sim$100 fs. A small part of the 800 nm beam is spectrally narrowed and serves as the visible beam. The energy of this pulse is 15 μJ and the bandwidth is $\sim$15 cm^{-1}. The LO-SFG signal is created by focusing the IR and VIS beams first on a metal surface. At the metal surface a relatively strong SFG signal is generated. This LO-SFG signal originates from a strong, but non-resonant $\chi^{(2)}$ of the metal. It should be noted that gold can only be used as a local oscillator for

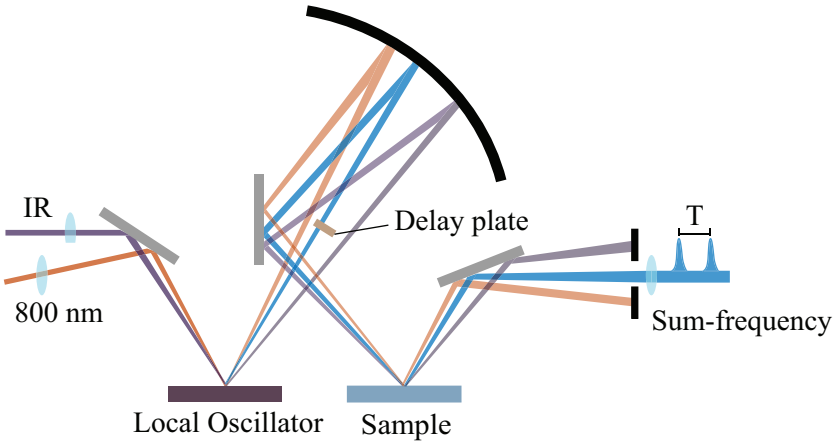

FIG. 1. Experimental lay-out of phase-sensitive vibrational sum-frequency generation (PS-SFG). A broadband femtosecond IR light pulse and a narrowband 800 nm pulse are focused onto a metal surface, generating an intense local oscillator SFG (LO-SFG) response that is delayed by a silica plate. The three beams are refocused onto the sample, producing an SFG signal that interferes with the LO-SFG signal on the CCD camera.

particular polarization combinations, because in the infrared region, metal surfaces generate a large electric field in the z direction and negligible fields in the x and y directions. As a result, the use of gold is limited to ssp and ppp polarization combinations. The spectral shape of the LO-SFG signal is a convolution of the spectra of the broad input IR pulse and the narrow-band visible pulse. This LO-SFG signal is sent through a silica plate to delay it in time with respect to the VIS and IR beams ($\sim$1.6 ps). The remaining IR and VIS beams are refocused with a parabolic mirror onto the sample interface to generate the sample VSFG signal. The LO-SFG and sample VSFG beams are collinear and coupled into a monochromator. The spectral interference pattern of the two SFG beams is detected with a Charge Coupled Device (CCD). The VSFG spectrum of the sample and the reference SFG signal of quartz need to be measured at the same height, as a difference in height would lead to a phase shift in the recorded spectra and thus in the phase of the extracted $\mathrm{Im}\chi^{(2)}$. The height of the sample is determined by monitoring the SFG signal on the CCD camera. A change in sample height leads to a translation of the SFG beam and thereby changes the position of the SFG signal on the CCD camera. We can determine the position of the SFG signal on the camera with a precision of 1 pixel size, which has 16 x 16 μm dimensions.

Taking into account the geometry of the optical SFG detection path, this converts into a precision of 20 μm for the determination of the height of the sample. As the infrared, visible and reference SFG beams travel nearly the same path, this accuracy suffices to keep the phase difference between the beams well defined. In previously reported implementations of heterodyne-detected VSFG spectroscopy, the LO-SFG beam was generated after the sample SFG[14,16]. This approach has a disadvantage that the LO-SFG signal needs to be corrected for the frequency-dependent reflectivity of the sample interface in the IR spectral region[17]. In the present method such a correction is not needed, as the LO-SFG beam is created before the VSFG signal of interest, and because the LO-SFG signal beam is generated with a metal surface for which the reflection is $\sim$100% for all frequency components contained in the IR pulse. Of course, in the used geometry the LO-SFG beam is reflected from the sample interface, but for the studied samples the reflectivity of this beam does not depend on frequency within its bandwidth.

We form hexane and heptane layers on a water surface by adsorption of the alkanes from their saturated vapors in a specially designed closed sample cell[20]. This method of sample preparation strongly reduces the risk of contaminations, because only volatile materials such as alkanes can evaporate and form a layer on water. The type of layer formed depends on a detailed balance between adhesive and cohesive forces. It has been found that short n-alkanes ($n \geq 4$) completely wet the surface, whereas alkanes with $5 < n < 8$ form an ultrathin layer with co-existing lenses on the water surface. Alkanes with $n > 8$ form only lenses and not a thin film[18,19]. The PDMS layer was formed by depositing $\sim$200 μl PDMS directly on the water surface, which resulted in a thin heterogeneous PDMS layer ($\sim$50-100 μm). PDMS is a hydrophobic polymer consisting of $(CH_3)_2SiO$ structural units and has a very low solubility in water, but due to its flexible backbone and weak intermolecular interactions between the methyl groups, it can wet the water surface. The chemical compounds D_2O ($\geq$99.96%, Cambridge Isotope Laboratories), n-hexane ($\geq$97.0%, Aldrich), heptane ($\geq$99.0%, Aldrich), NaOH (50% in water, Aldrich), HCL (1 M in water, Aldrich) and polydimethylsiloxane (PDMS, $M_r = 162.38$, $\geq$98.5%) were used as received.

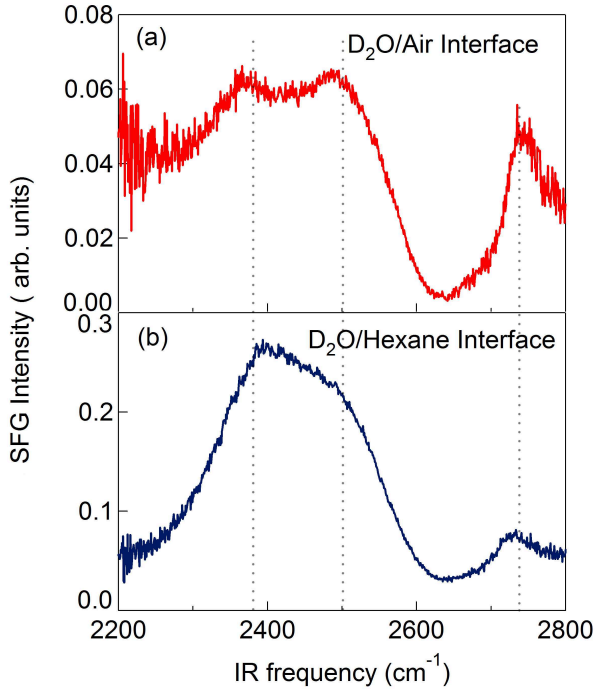

FIG. 2. Intensity vibrational sum-frequency generation (VSFG) spectra of (a) D_2O/air and (b) D_2O/Hexane; Both spectra are measured with an s-SFG, s-VIS, p-IR polarization combination).

III. RESULTS AND DISCUSSION

In figure 2 we present intensity VSFG spectra of D_2O/air and D_2O/hexane in the region of the OD stretch vibration. The D_2O/hexane interface generates a much stronger VSFG signal than D_2O/air. This finding shows that water molecules are much more strongly ordered at the interface with a hydrophobic liquid than at the interface with air. However, from these measurements it is not clear how the water molecules are oriented at the interface.

In figure 3 the real and imaginary part of $\chi^{(2)}$ ($\mathrm{Re}(\chi^{(2)})$ and $\mathrm{Im}(\chi^{(2)})$) are presented for D_2O/air and for three water/hydrophobic liquid interfaces. The $\mathrm{Im}(\chi^{(2)})$ spectrum of the D_2O/air interface shows a sharp positive feature at 2745 cm^{-1}, a broad negative band between 2400 and 2650 cm^{-1}, and a weak positive band between 2200 and 2400 cm^{-1}. This $\mathrm{Im}(\chi^{(2)})$ spectrum is in excellent agreement with the $\mathrm{Im}(\chi^{(2)})$ spectrum of the D_2O/air interface measured by Shen et al.[14] and Tahara et al.[16].

The sign of the $\mathrm{Im}(\chi^{(2)})$ depends on the orientation of the vibrational transition dipole with respect to the surface normal, meaning that a positive $\mathrm{Im}(\chi^{(2)})$ is associated with H_2O/D_2O molecules that have a net orientation of their hydrogen/deuterium atoms to-

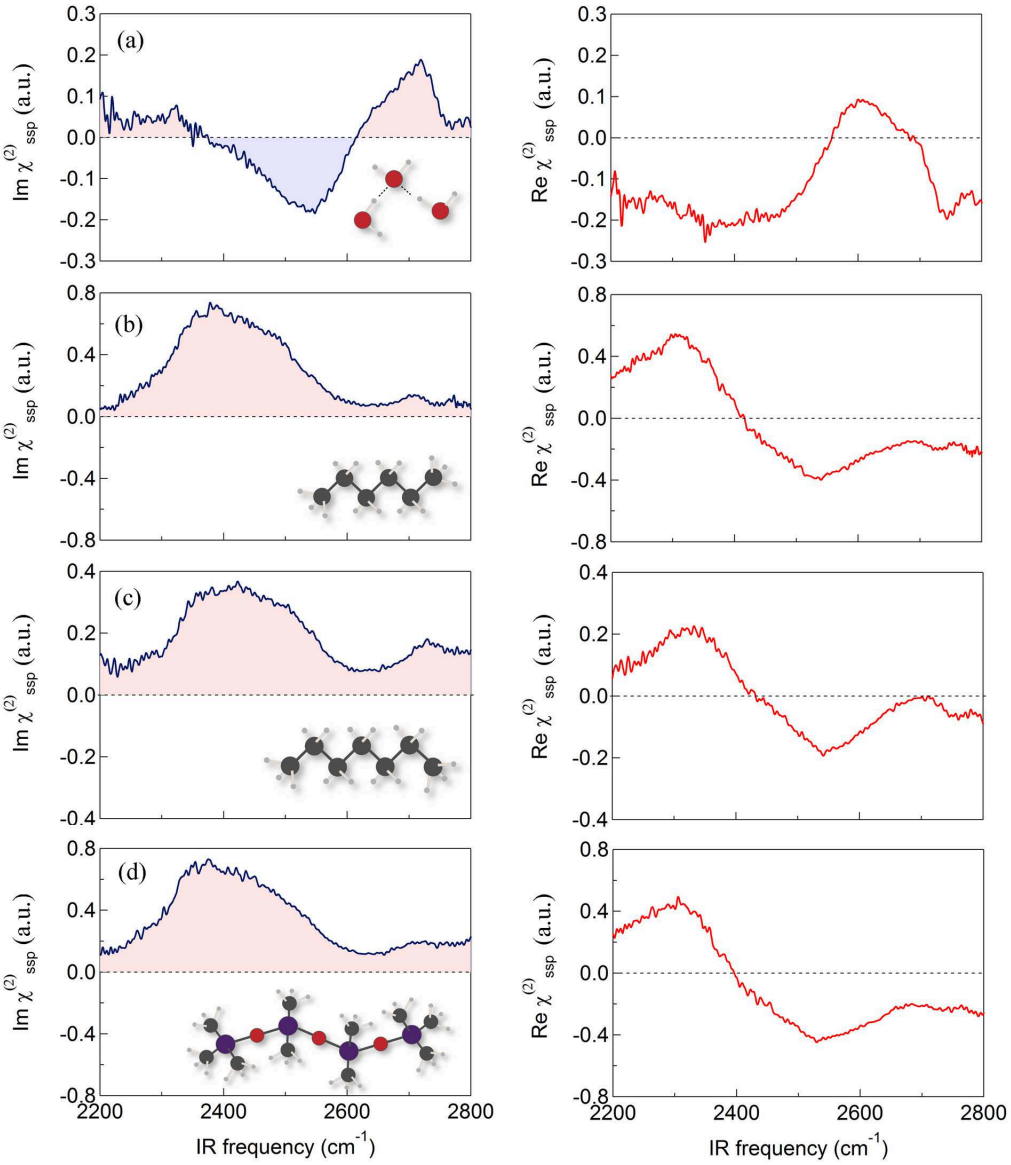

FIG. 3. Imaginary $\chi^{(2)}$ (blue) and real $\chi^{(2)}$ (red) parts of (a) D_2O/air, (b) D_2O/hexane, (c) D_2O/heptane, (d) D_2O/polydimethysiloxane. The spectra are measured with phase-sensitive VSFG spectroscopy with an s-SFG, s-VIS, and p-IR polarization combination.

wards the other phase, e.g. pointing away from the bulk of the water phase[11]. The positive band at 2745 cm^{-1} observed for the D_2O/air interface has thus been assigned to dangling OD groups pointing into air, and the negative part around 2500 cm^{-1} to hydrogen-bonded D_2O molecules with a net orientation of their OD groups towards the bulk liquid. The Im($\chi^{(2)}$)

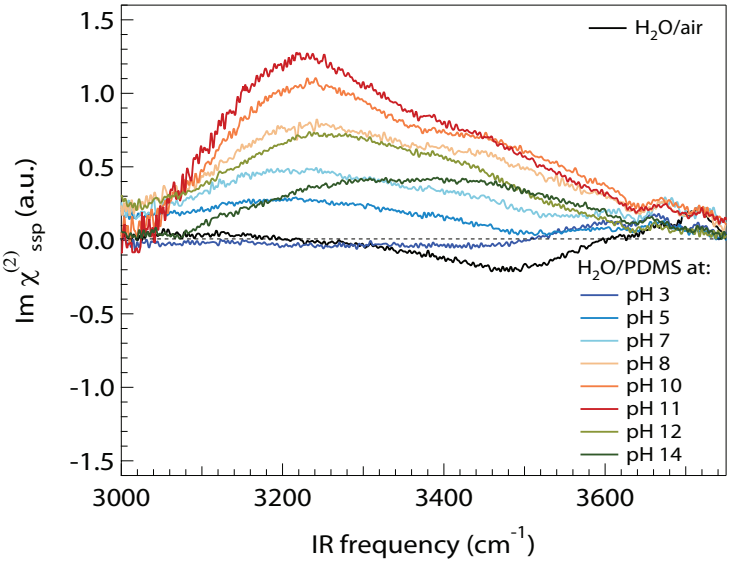

FIG. 4. Imaginary $\chi^{(2)}$ part of H_2O/polydimethysiloxane interface at different pH values (indicated in the legend).

spectrum also shows a weak positive band between 2200 and 2400 cm^{-1}. Pieniazek et al.[21] explained this positive band from the competition of the low-frequency contribution of four-hydrogen-bonded molecules with their O-H groups pointing to the interface. Ishiyama and Morita[22,23] presented a different explanation for the observation of a positive $\mathrm{Im}(\chi^{(2)})$ at low frequencies. According to this explanation the low-frequency vibration of a strongly hydrogen-bonded water molecule induces an oscillatory dipole moment in its hydrogen-bonded partner with a dipole orientation perpendicular to the surface. Hence, in this explanation the low-frequency part of $\mathrm{Im}(\chi^{(2)})$ is not assigned to single strongly hydrogen-bonded water molecules but rather to an anisotropic polarization coupling between different water molecules.

In figure 3 we show that the $\mathrm{Re}(\chi^{(2)})$ and $\mathrm{Im}(\chi^{(2)})$ spectra of the hydrophobe/water interfaces strongly differ from the corresponding spectra of the D_2O/air interface. For all hydrophobic interfaces $\mathrm{Im}(\chi^{(2)})$ is positive throughout the hydrogen-bonded band, indicating that the hydrogen-bonded O-D groups show a quite strong net orientation towards the hydrophobic phase. In addition, at low OD frequencies, there can also be a contribution from the anisotropic polarization effect that was proposed for the water/air interface[22].

Figure 4 presents $\mathrm{Im}(\chi^{(2)})$ spectra of H_2O/polydimethysiloxane (PDMS) at different pH values (ranging from pH 3 to pH 14). The pH was increased by adding NaOH and decreased

by adding HCl to the water phase. The results clearly show that changing the pH strongly affects the magnitude of $\mathrm{Im}(\chi^{(2)})$. With increasing pH, $\mathrm{Im}(\chi^{(2)})$ increases (becomes more positive), reaching a maximum value at ∼pH 11. This finding shows that at higher pH the water molecules become even more strongly oriented with their O-H groups pointing towards the oil phase than at neutral pH. Decreasing the pH below pH 7 leads to a decrease of $\mathrm{Im}(\chi^{(2)})$, meaning that water molecules become less oriented. At the lowest studied pH value of 3 the $\mathrm{Im}(\chi^{(2)})$ spectrum becomes even slightly negative over a large frequency of 3000 - 3500 cm^{-1}, indicating a net orientation of the water molecules with their O-H groups away from the oil phase.

The observation of a net orientation of water molecules near hydrophobic interfaces agrees well with previous experimental results[7,10] and the results of MD simulations of water/oil interfaces[10,24]. Both the experiments and simulations found the water molecules to be preferentially oriented with their O-H groups pointing towards the hydrophobic phase. In this study we investigate the properties of water/alkane interfaces and we observe that at all O-H stretch frequencies the water molecules show a net orientation with their O-H groups pointing towards the alkane phase. In a recent VSFG study by the group of Eric Tyrode it was found that the water ordering decreases if the water molecules are in direct contact with well packed self-assembled monolayers (SAM) of alkylsilanes adsorbed to silica surfaces[9]. This apparent difference with the present observations may be due to the fact that the SAM layers studied by Tyrode et al. show a molecular-scale structure that is quite different from the molecular-scale structure of the water/oil interfaces that we study. Probably, pure oil layers on water self-organize to a quite strongly corrugated surface that allows the hydrogen-bond network of water to fold around the protruding methyl groups. The SAM layers deposited on a silica surface studied by Tyrode et al. may be more flat on a molecular scale, thus being more similar to a hydrophobic solute with a large radius (>1 nm), for which it has been predicted that the hydrogen-bond structure of water is weakened[4].

The molecular-scale origin of the orientation of water molecules at an interface with alkane molecules has been a subject of intense debate. It has been proposed that this orientation arises from the presence of excess hydroxide ions at the water/oil interface[7]. As a result, the water/oil interface would possess a net negative charge, thereby inducing a preferred orientation of the O-H groups of water molecules in the adjacent layers towards the oil phase. The presence of excess hydroxide ions at the water/oil interface has also been

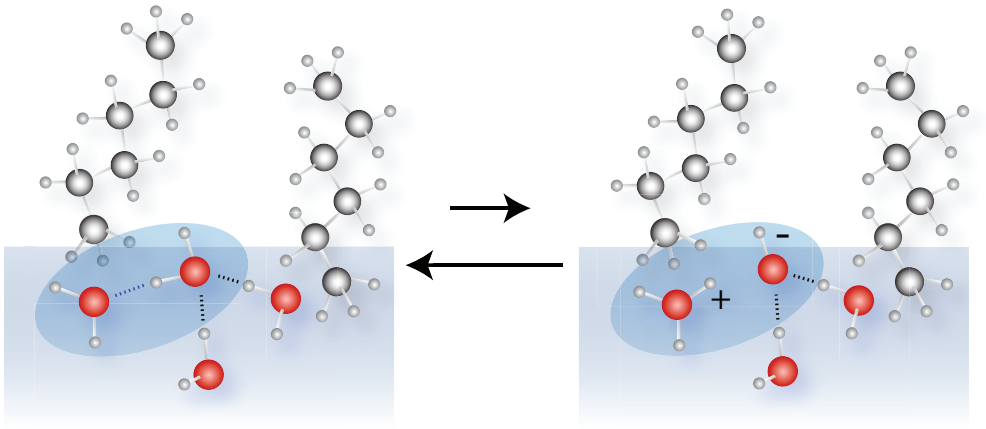

FIG. 5. Schematic illustration of the formation of a water/oil interface with the water O-H groups showing a net orientation to the hydrophobic layer.

proposed to be the origin of the observed negative ζ potential of oil droplets in water[25]. However, molecular dynamics simulations showed that the orientation of water molecules at water/alkane interfaces can also result from a purely structural effect, i.e. without invoking the presence of hydroxide ions[10,24]. In these simulations it was shown that there exists an imbalance in donating and accepting hydrogen bonds close to the interface, leading to a net orientation of the water dipole moments and O-H groups towards the hydrophobic phase. The imbalance in donating and accepting hydrogen bonds also gives rise to a local region of excess negative charge in the water phase at ∼0.5 nm from the Gibbs dividing surface.

The two explanations for the net orientation of water molecules at the interface of water and alkanes are not mutually exclusive. Both effects, i.e. excess hydroxide ions and structural effects, can be present and can even enhance each other. The imbalance in donating and accepting hydrogen bonds resulting from the truncation of the hydrogen-bond network will be accompanied by changes in the electron density. In a valence bond picture this would mean that the hydrogen-bonded $H_2O\cdots HOH$ pairs would have a stronger admixture of $H_2O^+H\cdots OH^-$ character, which would imply that the concentration of both hydronium (H_3O^+) and hydroxide (OH^-) would be increased near a water/alkane interface. In *ab initio* MD simulations of the water/air interface it was shown that the solvation structure of hydroxide ions is more flexible than that of hydronium and that the hydroxide ion becomes partially desolvated as it approaches the interface[26]. Moreover, the hydrogen bond donated by a hydroxide ion is weak, which implies that for a weakly hydrogen-bonded (dangling)

OH group at the interface the energy cost of acquiring OH^- character is smaller than for a strongly hydrogen-bonded OH group in the bulk. It is thus conceivable that the hydroxide character is more pronounced on the water OH groups that are in direct contact with the alkane molecules than on water OH groups that are deeper down in the water layer, meaning that an enhancement of the $H_2O^+H\cdots OH^-$ valence bond character would have a preferential orientation with the OH^- close to the alkane phase. This $H_2O^+H\cdots OH^-$ valence-bond character is further stabilized in case the OH group acquiring the OH^- character accepts two hydrogen bonds donated by H_2O molecule that are one layer deeper, as the formation of these hydrogen bonds is accompanied by a transfer of a small amount of negative charge from the hydrogen-bond accepting OH^- group to the two hydrogen-bond donating OH groups[10]. The configuration showing enhanced $H_2O^+H\cdots OH^-$ valence-bond character is schematically depicted in Fig. 5. An increase in $H_2O^+H\cdots OH^-$ valence-bond character at the interface will create a local electric field that orients nearby water OH groups towards the alkane phase. A similar orientation effect has been observed for sodium perchlorate solutions by the group of Heather Allen[27]. In this work it was shown that the small separation of the negative charges of the perchlorate ions (being closer to the surface) and the positive charges of the sodium ions (being further away from the surface) creates an electric field that orients water molecules in such a way that they have a net orientation of their O-H groups towards the interface.

This explanation is consistent with the observation that the orientation of water is further enhanced when the pH is increased, as shown in Figure 4. The higher bulk hydroxide concentration will stimulate the fraction of water molecules at the interface showing $H_2O^+H\cdots OH^-$ valence bond character, thereby increasing the local electric field that orients water OH groups towards the alkane phase. The surface concentration of $H_2O^+H\cdots OH^-$ valence bond structures will be very small (<<mmolar) and are thus not directly observable in the VSFG response. However, an increase in $H_2O^+H\cdots OH^-$ valence-bond character at the interface will create a local electric field that orients nearby water OH groups towards the alkane phase. As a result, $\mathrm{Im}(\chi^{(2)})$ acquires a positive sign at all frequencies, as is observed in Fig. 4.

Further *ab initio* molecular dynamics simulations will be needed to elucidate the potentially cooperative effect of local structure and charge redistribution on the hydrogen-bond structure and orientation of water molecules at the water-oil interface. These simula-

tions should specifically address water/oil interfaces, as we observe the properties of water molecules at these interfaces to be substantially different from that of water molecules at the water/air interface.

IV. CONCLUSIONS

We studied the structure and net orientation of water molecules at the water/hexane, water/heptane, and water/polydimethylsiloxane interfaces. With intensity vibrational surface sum-frequency generation (VSFG) spectroscopy we observe that the water hydrogen-bond structure at these interface is enhanced in comparison to the hydrogen-bond structure at the water/air interface. By interfering the VSFG light with the light of a local oscillator we determine the absolute phase of the VSFG light generated by the water/alkane and water/polydimethylsiloxane interfaces. Thereby we determine the orientation of the water molecules at all frequencies of the O-H stretch absorption spectrum. For all three studied interfaces the water molecules show a net orientation with their O-H groups pointing towards the hydrophobic phase. This net orientation is observed at all frequencies of the O-H stretch vibrational absorption spectrum. This behavior strongly differs from that of water molecules at the water/air interface, where the orientation depends on the O-H stretch frequency and where most hydrogen-bonded water molecules have their O-H groups pointing towards the water phase.

V. ACKNOWLEDGMENT

This work is part of the research program of the "Stichting voor Fundamenteel Onderzoek der Materie (FOM)", which is financially supported by the "Nederlandse organisatie voor Wetenschappelijk Onderzoek (NWO)". The work was performed within the framework of a FOM Industrial Partnership Program with Top-institute Wetsus for water research and is also financially supported by Wetsus.

REFERENCES

[1]H. S. Frank and J. W. Evans, *J. Chem. Phys.*, **13**, 507-532 (1945).

[2]A.K. Soper and J.L. Finney, *Phys. Rev. Lett.*, **71**, 4346-4349 (1993).

[3]S. Dixit, S.J. Crain, W.C.K. Poon, J.L. Finney, and A. K. Soper, *Nature*, **416**, 829-832 (2002).

[4]D. Chandler, *Nature*, **437**, 640-647 (2005).

[5]N. Galamba, *J. Phys. Chem*, **117**, 2153-2159 (2013).

[6]J. G. Davis, K. P. Gierszal, P. Wang, and D. Ben-Amotz, *Nature*, **491**, 582-585 (2012).

[7]C. S. Tian and Y. R. Shen, *Proc. Nat. Acad. Sic. USA*, **106**, 15148-15153 (2009).

[8]S. Ye, S. Nihonyanagi, K. Uosaki, *Phys. Chem. Chem. Phys.*, **3**, 3463-3469 (2001).

[9]E. Tyrode, J. F. D. Liljeblad, *J. Phys. Chem. C*, **117**, 17801790 (2013).

[10]R. Vacha, S. W. Rick, P. Jungwirth, A. G. F. de Beer, H. B. de Aguiar, J.-S. Samson, and S. Roke, *J. Am. Chem. Soc.*, **133**, 10201-10210 (2011).

[11]A. Morita and J. T. A. Hynes, *Chem. Phys. Lett.*, **258**, 371-390 (2000).

[12]Y.R. Shen, *Solid State Commun.*, **108**, 399-406 (1998).

[13]S. Nihonyanagi, J. A. Mondal, S. Yamaguchi, and T. Tahara, *Annu. Rev. Phys. Chem.*, **64**, 579-603 (2013).

[14]N. Ji, V. Ostroverkhov, C. S. Tian, and Y. R. Shen, *Phys. Rev. Lett.*, **100**, 096102 (2008).

[15]Y. R. Shen, *Annu. Rev. Phys. Chem.*, **64**, 129-50 (2013).

[16]S. Nihonyanagi, S. Yamaguchi, and T. Tahara, *J. Chem. Phys.*, **130**, 204704 (2009).

[17]R. E. Pool, J. Versluis, E. H. G. Backus, and Misha Bonn, *J. Phys. Chem.*, **115**, 15362-15369 (2011).

[18]T. Pfohl, H. Mohwald, and H. Riegler, *J. Phys. Chem.*, **14**, 52855291 (1998).

[19]O.-S. Kwon, H. Jing, K. Shin, X. Wang, and S. K. Satija, *Langmuir*, **23**, 1224912253 (2007).

[20]S. Strazdaite, J. Versluis, H. J. Bakker, *J. Chem. Phys.*, **140**, 054711 (2014).

[21]P. A. Pieniazek, C. J. Tainter, and J. L. Skinner, *J. Chem. Phys.*, **135**, 044701-11 (2011).

[22]T. Ishyiama and A. Morita, *J. Chem. Phys.*, **113**, 16299-16302 (2009).

[23]S. Nihonyanagi, T. Ishiyama, T. k. Lee, S. Yamaguchi, M. Bonn, A. Morita, and T. Tahara, *J. Am. Chem. Soc.*, **133**, 16875-16880 (2011).

[24]V. Knecht, H.J. Risselada, A.E. Markc, and S.J. Marrink, *J. Colloid Interface Sci.*, **318**, 477-486 (2008).

[25]P. Creux, J. Lachaise, A. Graciaa, and J. K. Beattie, *J. Phys. Chem. C*, **111**, 3753-3755 (2007).

[26]M.D. Baer, I-F.W. Kuo, D. J. Tobias, and C.J. Mundy, *J. Phys. Chem. B*, **118**, 8364-8372 (2014).

[27]W. Hua, D. Verreault, and H. C. Allen, *J. Phys. Chem. Lett.*, **4**, 4231-4236 (2013).